Available online at www.sciencedirect.com
ScienceDirect
Carbohydrate Polymers 71 (2008) 159–169
Carbohydrate Polymers
www.elsevier.com/locate/carbpol

Isolation and characterization of an acidic polysaccharide from *Mesona Blumes* gum

Feng Tao, Gu Zheng Biao *, Jin Zheng Yu, Zhuang Hai Ning

Key Laboratory of Food Science and Safety of Education Ministry, School of Food Science and Technology, Southern Yangtze University, No.1800 at Lihu Road, Jiangsu, Wuxi 214122, PR China

Received 7 August 2006; received in revised form 10 April 2007; accepted 4 May 2007
Available online 18 May 2007

Abstract

A neutral polysaccharide (NMBG) and an acidic polysaccharide (AMBG) were fractionated from *Mesona Blumes* gum (MBG) with yields of 0.5% and 90% (w/w), respectively. AMBG was composed of Gal, Glc, Man, Xyl, Ara, Rha and GalA with a molar ratio of 2.66:1:0.37:2.29:12.5:5.99:23.5, and NMBG consisted of Gal, Glc, Man, Xyl, Ara, Rha with a molar ratio of 9.9:15.3:4.31:1.48:11.6:1. But there was no GalA in NMBG. Both AMBG and NMBG were homogeneous with Mw of 6566 and 5277, respectively. AMBG could form a viscous solution but NMBG could not. Structure features of the purified AMBG were investigated by a combination of chemical and instrumental analyses, such as periodate oxidation, Smith degradation, GC–MS, ^{13}C and ^{1}H NMR. It was found that AMBG possessed a α-(1 → 4)-galacturonan backbone with some insertions of α-1,2-Rha*p* residues. The branches of arabinogalactan, arabinan, galactan and xylan could be all attached to the backbone via O-4 of Rha*p* residues. In addition, some Rha*p* residues on the backbone terminated with α-L-Ara*f* and some O-6 in galacturonic acid residues could be acetylated and some O-6 in GalA*p* residues could be methyl estered. The molecular structure of AMBG at different concentrations was observed with atomic force microscopy (AFM). AMBG showed a spherical lump at 1 μg/mL, but an irregular shape like worm at 10 μg/mL, which indicated that the viscous property of AMBG might be caused by its strong tendency to aggregate.

Keywords: *Mesona Blumes* gum; Molecular weight; Monosaccharide component; Periodate oxidation; Smith degradation; GC–MS; ^{13}C and ^{1}H NMR; AFM

1. Introduction

Mesona Blumes is a herb from Lamiaceae family originally from South China and wide spread in Southeast Asia. In China, it has been used as a folk medicine for preventing heatstroke, hypertension, diabetes and muscle or joint pain. The unique aroma and health benefits of this herb make it popular to the Chinese. Traditionally the plant is consumed as a herbal tea or as a jelly-type dessert (a mixed gel with non-waxy type starch) (Lai & Lin, 2004).

Mesona Blumes contains an ionic polysaccharide gum, named *Mesona Blumes* gum (MBG). As compared with other commercial gums, MBG forms a low-viscosity solution with pronounced shearing-thinning behaviour (Lai, Tung, & Lin, 2000). Although the structural features of MBG are still unclear, Yang and Huang (1990) reported that the core of the structure was a heteroglycan, containing galactose, glucose, rhamnose, arabinose and uronic acid with a molar ratio of about 2:1:1:1:2. Lai, Liu, and Lin (2003) reported that the neutral sugar composition of crude MBG could be rhamnose, arabinose, galactose, glucose, xylose, mannose, fructose and erythrose at mole fraction of 13.68%, 10.26%, 20.86%, 23.25%, 6.84%, 14.71%, 10.26% and 0.14%, respectively, but the uronic acid content is not reported.

Polysaccharide gums have wide applications because of their rheological properties. Although MBG has a unique rheological property, there is lack of systematic structural analysis. In order to elucidate the relationship between the rheological characteristics of MBG and its structure,

* Corresponding author. Tel.: +86 510 85913653; fax: +86 510 85913653.
E-mail address: ggzb@sohu.com (G. Zheng Biao).

0144-8617/$ - see front matter © 2007 Published by Elsevier Ltd.
doi:10.1016/j.carbpol.2007.05.017

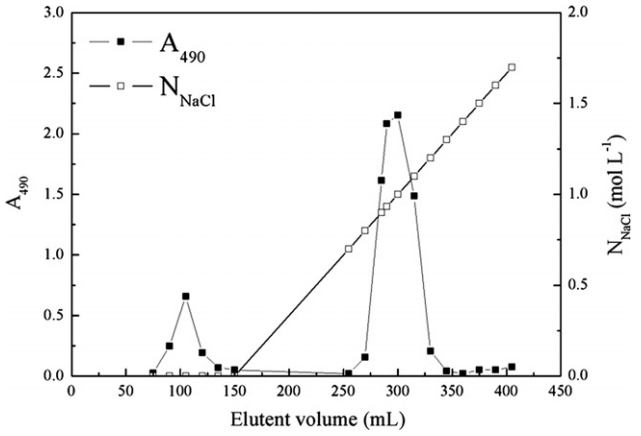

Fig. 1. Elution profile of MBG on DEAE-Sepharose Fast Flow (D2.6 × 50 cm).

this work describes: (a) isolation and purification of MBG; (b) molecular weight determination of MBG by High Performance Gel Permeation Chromatography (HPGPC); (c) structural characterization of MBG by periodate oxidation, Smith degradation, methylation analysis, UV, IR and NMR spectroscopy; and (d) clarification of the monosaccharide component and the bond structure in the MBG.

2. Materials and methods

2.1. Materials

Crude MBG was kindly donated by a Fujian farmer. DEAE Sepharose Fast Flow was bought from Pharmacia Biotech Ltd. (Denmark); D-mannose, D-Galactose,

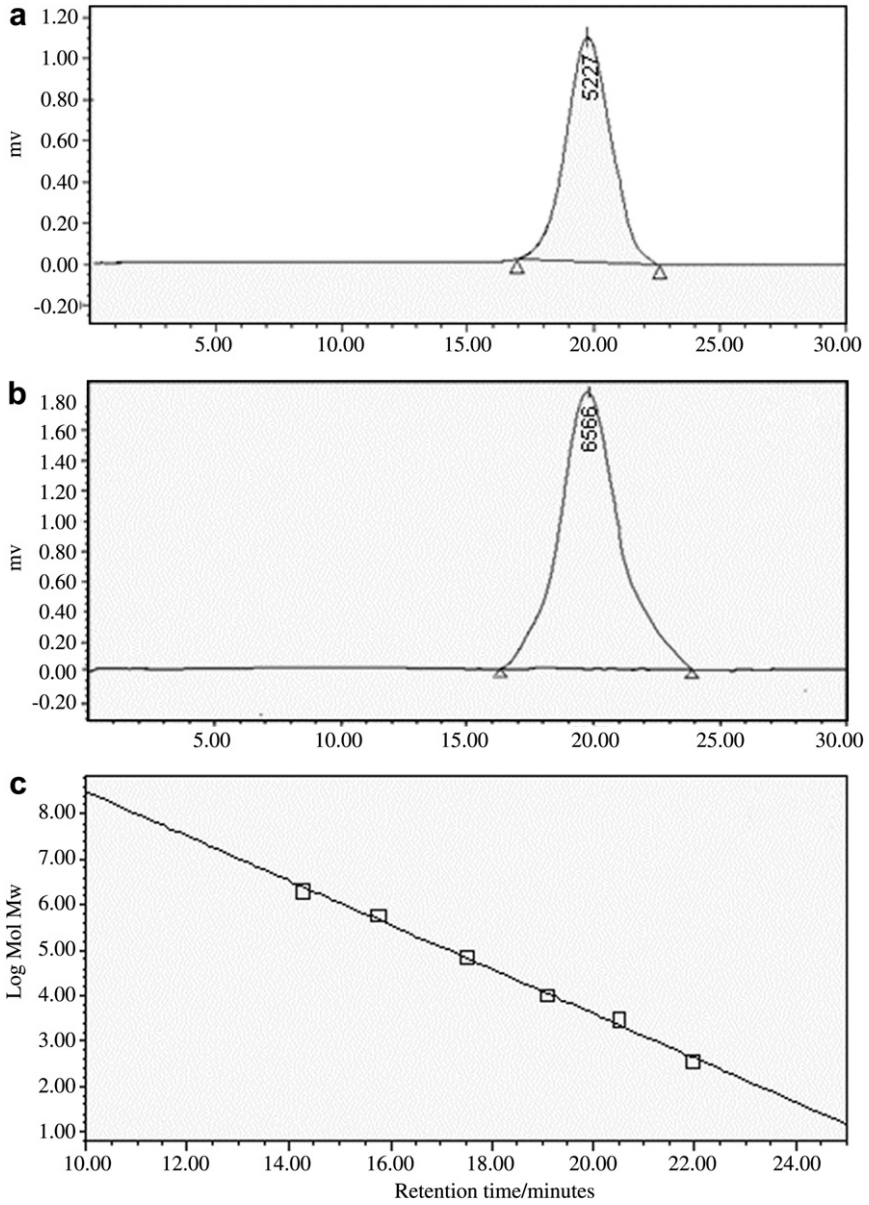

Fig. 2. HPGPC chromatograms on Ultrahydrogel column of (a) NMBG (b) AMBG. (c) Calibration standard curves of lgMw and relative retention time (t) of Dextran T on Ultrahydrogel. The linear fit equation of this standard curve was lg Mw = 13.7 − 0.499t, $R^2 = 0.9974$.

D-Glucose, D-xylose, L-rhamnose, D-ribose, D-arabinose and L-fucose were bought from Sigma Chemical (USA); Dextran standard series T-2000, T-580, T-188, T-70, T-10 and T-5 were bought from Pharmacosmos Co. Ltd. (Denmark); the other analytically pure reagents were bought from the Shanghai Chemical Reagent (PR China).

2.2. Isolation and purification of MBG

The dried MBG (200 mg) was dissolved in 25 mL, pH 6.0, 0.02 mol/L phosphate buffer, and was further purified on a DEAE-Sepharose Fast Flow gel column ($\Phi 2.6 \times 50$ cm), firstly by using pH 6.0, 0.02 mol/L phosphorous buffer and then using 2 mol/L sodium chloride in pH 6.0, 0.02 mol/L phosphorous buffer as gradient eluent at a flow rate of 2.5 mL/min. Each tube was collected every 2 min and the fractions were analyzed by the phenol–sulfuric acid method (Zhang, Yao, Chen, & Wang, 2007).

2.3. Homogeneity and molecular weight of MBG

The homogeneity and molecular weight of MBG were determined by Gel Permeation Chromatography (GPC) with a Waters HPLC apparatus (Waters 600, Waters Co. Ltd., USA) equipped with an ultrahydrogel™ column (300×7.5 mm), a model 2410 Refractive index detector. A Millennium-32 Workstation was used for the calculation of average molecular weights. The dextran standards (T-2000, T-580, T-188, T-70, T-10 and T-5) were used to calibrate the column. The detailed operation conditions were mobile phase: 0.1 mol/L sodium nitrate; flow rate: 0.9 mL/min; column temperature: 45 °C; column pressure: 5 MPa (model 600 pump); injection volume: 50.00 μL; sampling volume: 20.00 μL; running time: 40 min (Liu et al., 2007).

2.4. General analysis methods of NMBG and AMBG

Ultraviolet spectra were recorded with a UV/Vis2000 spectrometer (Ruili Co. Ltd., Beijing, PR China), and infrared spectra were measured on an Nicolet 5DXB FT-IR infrared spectrometer (Nicolet Co. Ltd., USA) and then analyzed with OMNIC 2.1 software. Monosaccharide composition was measured according to the following procedure: purified neutral MBG(NMBG) and Acidic MBG(AMBG) 30 mg were firstly dissolved into 5 mL 2 M trifluoroacetic acid, respectively, then both AMBG and NMBG solution were heated at 121 °C for 1 h. After cooling, the solution was centrifuged at 10,000*g*. The supernatant was concentrated by rotary evaporation and then freeze-dried. The dried sample was derivatized into alditol acetates in the usual way and subjected to HPLC analysis. The following sugars were used as references: D-glucose, D-xylose, D-mannose, D-galactose, D-rhamnose, L-fucose, D-arabinose and D-galacturonic acid (Caili, Haijun, Tongyi, Yi, & Quanhong, 2007). The steady shear viscosities of NMBG and AMBG (1–5%, w/w) were determined using the parallel-plate system of an AR1000 rheometer at 25 °C. The detailed operation conditions were: plate diameter 4 cm, gap between plates 500 μm, and the shear rate was 1–100 s^{-1} (Kjoniksen, Hiorth, & Nystrom, 2005).

2.5. Periodate oxidation and smith degradation of AMBG

A suspension of AMBG (50 mg) in 0.015 mol/L sodium metaperiodate (50 mL) was kept stirring at 4 °C in the dark. At intervals, the periodate consumption was determined with the Fleury–Lange method (Fleury & Lange, 1933). After the consumption of periodate was kept constant (10 days), excess of periodate was reduced with ethylene glycol and the liberated formic acid was titrated with 0.01 mol/L sodium hydroxide. Oxidized product was dia-

Table 1
Monosaccharide composition of NMBG and AMBG (calculated as mole percentage)

Mole percentage	Gal	Glc	Man	Xyl	Ara	GalA	Rha
NMBG (%)	22.75	34.99	9.88	3.39	26.69	–	2.29
AMBG (%)	5.51	2.07	0.77	4.75	25.88	48.62	12.4

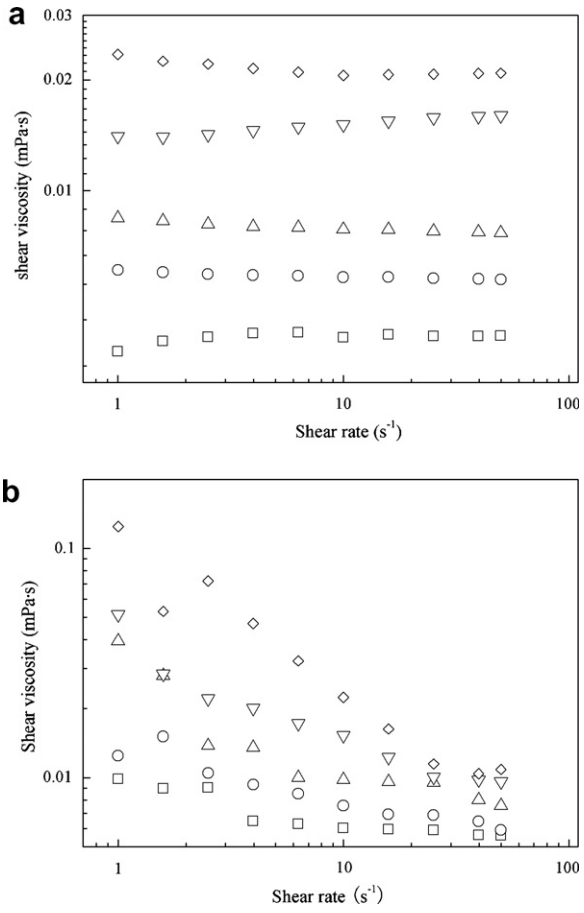

Fig. 3. Steady shear rheology of (a) 1–5% (w/w) NMBG and (b) 1–5% (w/w) AMBG at shear rates 1–100 s^{-1} at 25 °C. □ 1%, ○ 2%, △ 3%, ▽ 4%, ◇ 5%.

lyzed against tap-water (2 days) and distilled water (1 day), the residue in the dialysis bag was filtered, re-dissolved in distilled water (20 mL), reduced with sodium borohydride, and the reduced solution was decomposed by the addition of 10% acetic acid to pH 5.5. The reaction mixture was dialyzed against tap-water and distilled water and filtered, after lyophilization a white powder of AMBG polyalcohol (AMBG-1) was obtained. AMBG-1(10 mg) was hydrolyzed with 2 M trifluoroacetic acid (2 mL) at 121 °C, 0.1 MPa for 1 h in sealed tubes, and the mixture was evaporated to dryness. The sugars or alcohols thus obtained were converted into their alditol acetates and subjected to gas chromatography analysis. Gas chromatography was conducted on a Shimadzu GC-14A gas chromatograph (Japan Shimadzu Co., Tokyo, Japan) equipped with a SPB-5 column (30 m × 0.53 mm) and a flame ionization detector. The detailed experimental conditions were: H_2 (30 mL/min); air (200 mL/min); N_2 (20 mL/min); the initial column temperature of 150 °C was held for 1 min and then the temperature was increased at 10 °C min^{-1} to 205 °C in 5.5 min, held at 205 °C for 1 min and then increased again at 3 °C min^{-1} to 240 °C, held for 20 min. The temperature of the injector was 205 °C and the temperature of the detector was 240 °C. D-glucose, D-xylose, D-mannose, D-galactose, D-rhamnose, L-fucose, D-arabinose, glycerol and erythritol were used as references. Inositol was used as an internal standard (Duan, Zheng, Dong, & Fang, 2004).

2.6. Methylation analysis

Methylation of AMBG was carried out in three stages. Firstly, the uronic acids of AMBG were reduced to the corresponding neutral sugars: AMBG (5 mg) was fully solubilized in D_2O at pH 4.75, then carboxyl esters were first reduced with sodium borodeuteride in imidazole buffer to generate 6,6-dideuteriosugars, while free uronic acids were activated with a carbodiimide (*N*-cyclohexyl-*N*′-(2-morpholinoethyl)-carbodiimide methyl-*p*-toluenesulfonate, Sigma–Aldrich) and it was then reduced with sodium borodeuteride, dialyzed and freeze-dried as previously described (Taylor & Conrad, 1972; Ciucanu & kerek, 1984). Secondly, carboxyl-reduced AMBG (3 mg) was fully solubilized in DMSO, reacted with sodium hydroxide powder and methyl iodide. After that, the reaction solution was extracted by methyl iodide and poured through a Na_2SO_4 column, then the filtrate was collected and volatilized with nitrogen as described by Ciucanu and kerek, 1984. Thirdly, methylated AMBG was hydrolyzed with 2 M trifluoroacetic acid and reduced with sodium borodeuteride, then 0.5 mL acetic anhydride was added and derivatized at 100 °C. The derivatives were partially methylated alditol acetates (PMAA). The methylated polysaccharides were examined with FT-IR spectroscopy. Complete methylation was confirmed by the lack of a hydroxyl peak. The resulting PMAA were subjected to GC–MS analysis. Analyses were performed on a GC (GC-14A, Shimadzu, Japan) interfaced with a MS (Finnigan Trace MS, Finnigan Co., USA) mass-selective detector at 70 eV ionization energy. The GC column was an OV1701 (30 m × 0.25 mm), with a temperature program from 150 to 250 °C at a rate of 3 °C min^{-1}. The rate of helium carrier gas was 3.0 mL/min. The interface temperature was 250 °C, the ion source temperature was 200 °C and the detective voltage was 350 V. The quantification for the molar ratio of each sugar was calibrated using the peak area and response factor of the FID in GC (Shiga & Lajolo, 2006).

2.7. Nuclear magnetic resonance (NMR) spectroscopy

^1H experiments were performed on a Bruker Avance 400 spectrometer (operating frequency of 400.13 MHz). Samples were examined as a solution in D_2O at 333 K in a 5 mm i.d. tube (internal acetone ^1H (CH_3) at 2.1 ppm relative to Me_4Si). ^{13}C NMR experiments were conducted on the same spectrometer (operating frequency: 100.57 MHz). Sample data were recorded as a solution in D_2O at 333 K in a 5 mm i.d. tube (internal acetone ^{13}C (CH_3) at 31.5 ppm relative to Me_4Si) (Habibi, Heyraud, Mahrouz, & Vignon, 2004).

2.8. Atomic force micrograph (AFM)

AMBG solution (1 mg/mL) was prepared by adding some purified AMBG into double distilled H_2O. The aqueous solution was stirred for about 1 h at 80 °C in a sealed bottle under N_2 stream so that AMBG dissolved completely. After cooling to room temperature, the solution was diluted to the final concentration of 1 and 10 μg/mL. About 10 μL of diluted AMBG solution was dropped on the surface of a mica sample carrier, allowed to dry (Kirby, Gunning, & Morris, 1995), and then was imaged in air at room temperature. The atomic force microscopy used in this study was a Nano Scope IIIa (Digital Instruments, DI Co., USA) and was operated in the tapping-mode. The resulting imaging force was estimated to be 3–4 nN and the resonant frequency was about 2 kHz (Gunning et al., 2003).

3. Results and discussion

3.1. Isolation, purification and general properties of MBG

MBG was separated into two fractions on DEAE Sepharose Fast Flow (Fig. 1). NMBG was eluted at 0 mol/L sodium ion concentration while AMBG was eluted at 0.6–0.7 mol/L sodium ion concentration. The yield of NMBG was 0.5% while that of AMBG was 90% based on crude MBG. Both NMBG and AMBG are white powder, soluble in hot water with characteristic absorption of polysaccharide at 190 nm, and no absorption at 280 and 260 nm for protein and nucleic acid. HPGPC of either NMBG or AMBG gave a single and symmetrical peak (Fig. 2a and b). With Dextran standards being used to make the calibration curve (Fig. 2c), the average molecular weight of NMBG and AMBG were 5277 and

6566 Da, respectively. NMBG showed IR absorptions at 872 cm^{-1} (β-configuration), 1066 cm^{-1}, 1138 cm^{-1} (pyranoside), 1646 cm^{-1} ($\nu_{C=0}$), 2930 cm^{-1} (ν_{C-H}), 3406 cm^{-1} (ν_{O-H}), and no absorption at 756 cm^{-1} for the α-configuration, which indicated that NMBG might consist of β-pyranoside. AMBG exhibited IR absorptions at 896 cm^{-1} (β-configuration), 758 cm^{-1} (α-configuration), 1105 cm^{-1}, 1143 cm^{-1} (pyranoside), 1621 cm^{-1} ($\nu_{C=0}$), 2924 cm^{-1} (ν_{C-H}), 3403 cm^{-1} (ν_{O-H}), indicating that AMBG might consist of both α-configuration and β-configuration. As shown in Table 1, monosaccharide components of NMBG in mole ratio were Gal:Glc:Man:Xyl:Ara:Rha = 9.9:15.3:4.31:1.48:11.6:1 while those of AMBG in mole ratio were Gal:Glc:Man:Xyl:Ara:Rha:GlaA = 2.66:1:0.37:2.29:12.5:5.99:23.5. NMBG had no galacturonic acid but AMBG contained it. Moreover, it was found that NMBG solutions (1–5%) all exhibited a Newtonian flow behavior (Fig. 3a) and AMBG solutions (1–5%) all exhibited a shear-thinning flow behavior (Fig. 3b) under the shear rate range from 1 to 100 s^{-1}. Hence in order to explore the relationship between the structure and rheological properties, AMBG was selected to perform further investigation on its exquisite structure.

3.2. Periodate oxidation analysis and smith degradation products of AMBG

The oxidation of AMBG with 0.015 mol/L sodium periodate at 4 °C was completed in 8 days, the consumed periodate and the liberated formic acid were 0.99 and 0.125 mol/mol of monosaccharide residue, respectively. Formic acid was formed after periodate oxidation of AMBG, which indicated that hexapyranose with $1\rightarrow$, $1\rightarrow6$ glycosyl linkage probably existed. The amount of consumed periodate was twice that of the formed formic acid, which indicated that a lot of glycosyl linkages which only consumed periodate but formed no formic acid still existed, as for hexapyranose, $1\rightarrow2$, $1\rightarrow2$, 6, $1\rightarrow4$, $1\rightarrow4$, 6 probably existed, as for furanose, $1\rightarrow$, $1\rightarrow5$ probably existed. The oxidized AMBG was reduced with sodium borohydride to give the corresponding polyalcohol (AMBG-1). AMBG-1 was completely hydrolyzed with acid. The hydrolyzed products were converted into their alditol acetates; GC analysis indicated the presence of glycerol, erythritol and monosaccharides (Fig. 4c). The amount of glycerol detected was about 70% (mole percentage), which indicated that a lot of hexapyranose with $1\rightarrow$, $1\rightarrow6$, $1\rightarrow2$, $1\rightarrow2$, 6 glycosyl linkages existed in AMBG. While the amount of erythritol detected was about 3.61%, which indicated that a few hexapyranose with $1\rightarrow4$, $1\rightarrow4$, 6 glycosyl linkages existed in AMBG. The reducing product of galacturonic acid with $1\rightarrow4$ glycosyl linkage was fully hydrolyzed into glyoxal or ethylene glycol. In addition, the retained residues of arabinose and galactose demonstrated that side chains of the hairy regions were resistant to periodate oxidation. An occurrence of the rhamnose residues in the fragment AMBG-1 indicated that some of these residues appeared to be substituted with side chains (Bushneva, Ovodova, Shashkov, & Ovodov, 2002).

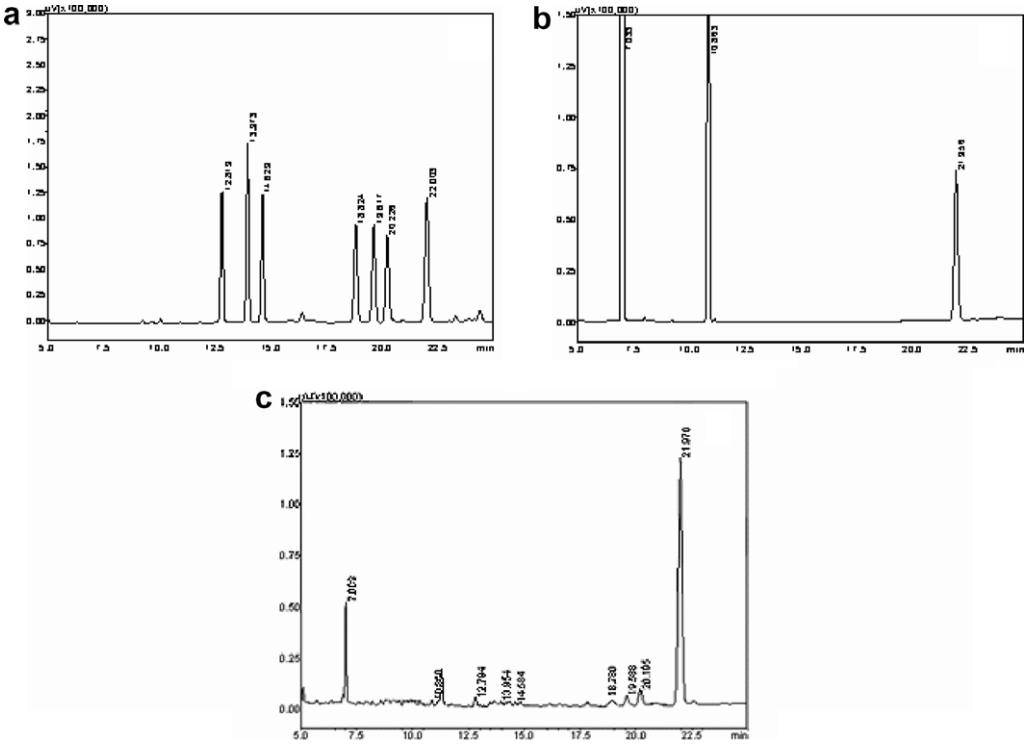

Fig. 4. GC chromatography of (a) monosaccharide and internal standard, Rha, Ara, Xyl, Man, Glc, Gla and inositol (from left to right), (b) polyalcohol and internal standard, glycerol, erithritol and inositol (from left to right), (c) smith degraded production of AMBG.

3.3. Methylation results of AMBG

Carbodiimide-activated reduction of the carboxyl groups of glycosyluronic acids with sodium borodeuteride ($NaBD_4$) resulted in an easily identified sugar (deuterized). There was only one major peak detected from the GC–MS analysis of the partially methylated alditol acetate (PMAA) derived from the carboxyl reduced AMBG as shown in Fig. 5a, and its corresponding mass spectrum is displayed in Fig. 5b. The combination of the fragmentation pattern and retention time of the PMAA suggested that the reduced polysaccharide was made of 1,4-linked D-galactosyl residues. Combined with the results of monosaccharide components, it was assumed that the major peak in Fig. 5a represented 4-***O***-substituted D-galacturonic acid. This result indicates that AMBG is probably a pectin which has a linear backbone chain of $1 \rightarrow 4$-linked α-D-galacturonic acid units (Singthong, Cui, Ningsanond, & Douglas, 2004). Methylation results are given in Table 2, it was concluded from Table 2 that: (a) AMBG was mainly composed of 1,4-D-Gal*p*A, T-,1,6-,1,3,6-,1,4-,1,4,6,-D-Gal*p*, T-,1,5-,1,3,5-L-Ara*f*, 1,2-,1,2,4-L-Rha*p*, T-,1,4-D-Xyl*p*,

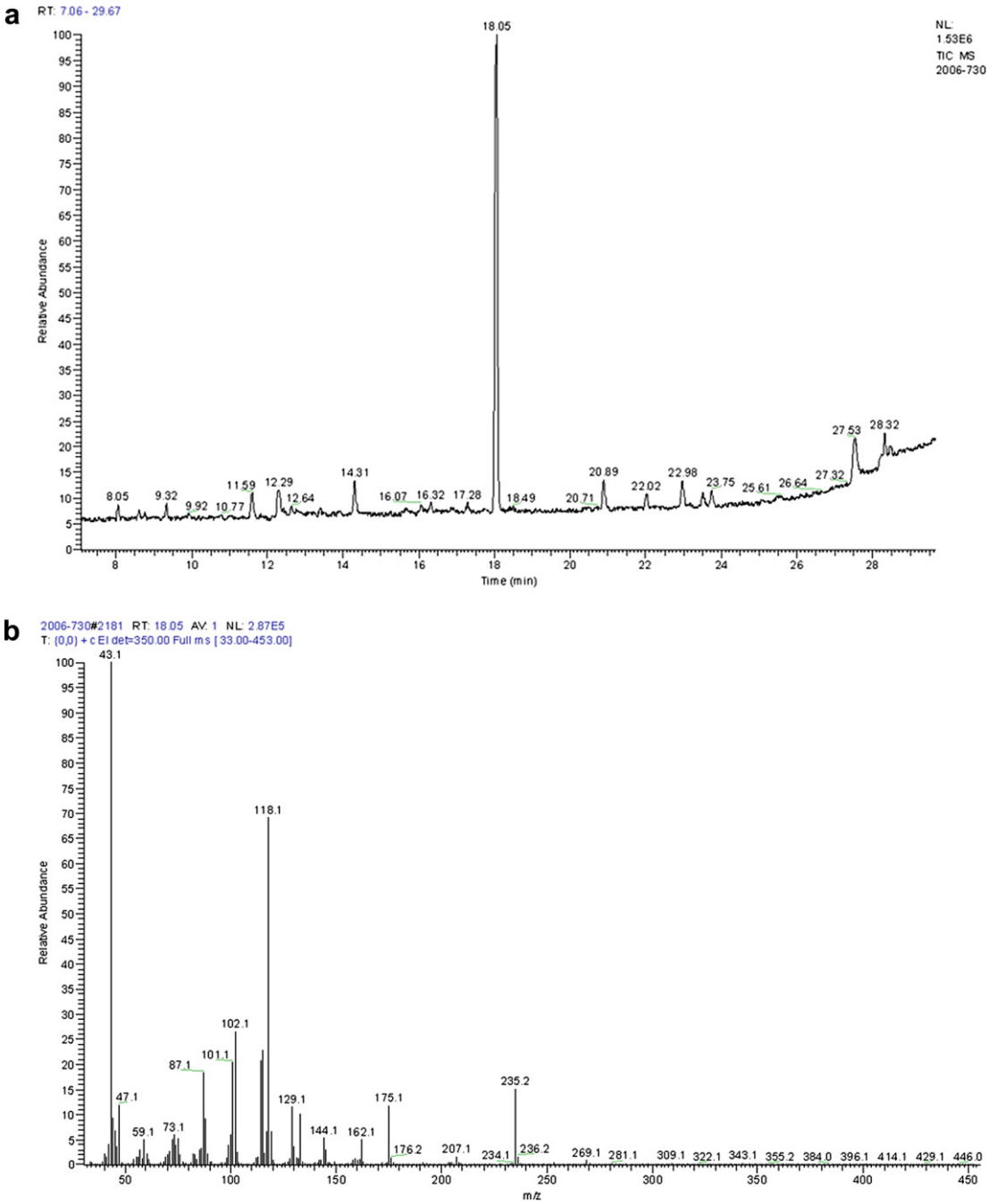

Fig. 5. (a) Reconstructed total ion chromatograph of carboxyl-reduced and methylated AMBG. (b) Mass spectrum of peak $RT_{18.05}$ (1,4-GalA) in (a).

1,2-D-Man*p*, T-,1,4-D-Glc*p*; (b) rhamnose residues were mainly linked with 1 → 2 glycosidic linkage. Oxygen substitution at the fourth site of Rha*p* (20.6%) would take place and turn into 1,2,4-Rha*p*; (c) the mole ratio of T-,1,5-,1,3,5-L-Ara*f* was 35.3:36.8:27.9, the backbone of arabinan consisted of Ara*f* (64.7%) residues with 1 → 5 glycosidic linkage. There were branched chains linked with the oxygen atom at the third site of Ara*f* residues (33.3%), which indicated that its branched degree was relatively high. The other Ara*f* residues (about 35.3%) existed as non-reduced ends, which indicated that all T-Ara*f* were not linked with arabinan, they could locate in galactan branch or directly in the backbone of AMBG; (d) the mole ratio of T-,1,6-,1,3,6-,1,4-,1,4,6,-D-Gal*p* was 37.8:34.3:18.7:4.0:5.2, i.e., Gal*p* residue (58.2%) was mainly linked by 1 → 6 glycosidic linkage. Branched chains linked with the oxygen atom at the third site of Gal*p* residue (18.7%). In addition, some Gal*p* residues (4.0%) was linked with 1 → 4 glycosidic linkage, the other Gal*p* residues (37.8%) existed as non-reduced ends; (e) Gal*p*A was the main glycosyl unit of AMBG. There were about 99.3% Gal*p*A residues linked with 1 → 4 glycosidic linkage and 0.7% Gal*p*A residues existed as non-reduced ends. Moreover, there were very few amounts of D-Glc*p*, D-Xyl*p* and D-Man*p* in AMBG (Inngjerdingen et al., 2005; Li, Nakagawa, Nevins, & Sakurai, 2006).

3.4. NMR results of AMBG

Signals in the ^{1}H NMR (Fig. 6a) and ^{13}C NMR (Fig. 6b) spectra of the AMBG were assigned as completely as possible, based on periodate oxidation, methylation analysis and on literature values. The ^{1}H NMR of AMBG showed resonances corresponding to a C-methyl proton at δ 1.90 and δ 2.02 and anomeric protons δ 5.95 due to the α-Ara*f* residues. Weak signals at δ 1.08 and δ 1.13 were attributed to methyl proton of Rha*p* residues; this signal usually appeared as two widely separated pair peaks, which indicated that there were two kinds of glycosyl linkages of Rha*p* residues. H-1 signals were assigned to the α-Rha*p* residues (4.56), the α-GalA*p* residues (4.95), the β-Xyl*p* residues (4.74) and the β-Gal*p* residues (4.28), respectively (Cozzolino et al., 2006).

The ^{13}C NMR spectra of AMBG identified signals of the ***O***-methyl as carboxylic acid methyl esters at δ 55.45, the carboxyl, in acidic form at δ 178.3 and the carboxyl, in ester-form at δ 173.6. In the anomeric carbon region, signals at δ 102.9 could be attributed to C-1 of α-Ara*f*; δ 102.1 to C-1 of β-Gal*p*; δ 101.7 to C-1 of β-Xyl*p*; δ 101.5 to C-1 of α-Gal*p*A, respectively (Sims & Newman, 2006). The mythylene signals of C-5 of Ara*f*, Xyl*p* and C-6 of Gal*p* residues were identified by the application of DEPT ^{13}C NMR analysis, in which they appeared as negative peaks. δ 62.8

Table 2
Methylation analysis of AMBG

Monosaccharide residues	Glycosyl linkage	Methylated sugar	Mol. %[b]	Mol. %[c]	Retention time (min)
L-Rha*p*	1,2-	3,4-Me_2-Rha*p*	79.4		12.29
	1,2,4-	3-Me-Rha*p*	20.6		16.32
	Total		100.0	6.06	
L-Ara*f*	T-	2,3,5-Me_3-Ara*f*	35.3		8.05
	1,5-	2,3-Me_2-Ara*f*	36.8		12.64
	1,3,5-	2-Me-Ara*f*	27.9		16.07
	Total		100.0	3.76	
D-Xyl*p*	T-	2,3,4-Me_3-Xyl*p*	35.9		9.33
	1,4-	2,3-Me_2-Xyl*p*	64.1		23.75
	Total		100.0	3.98	
D-Man*p*	T-	2,3,4,6-Me_3-Man*p*	100.0		22.02
	Total		100.0	1.87	
D-Gal*p*	T-	2,3,4,6-Me_4-Gal*p*	37.8		14.31
	1,6-	2,3,4-Me_3-Gal*p*	34.3		20.89
	1,3,6-	2,4-Me_2-Gal*p*	18.7		27.03
	1,4-	2,3,6-Me_2-Gal*p*	4.0		26.25
	1,4,6-	2,6-Me_3-Gal*p*	5.2		28.47
	Total		100.0	12.12	
D-Glc*p*	T-	2,3,4,6-Me_4-Glc*p*	60.8		23.52
	1,4-	2,3,6-Me_3-Glc*p*	39.2		18.49
	Total		100.0	2.64	
D-Gal*p*A[a]	T-	2,3,4,6-Me_4-Gal*p*(6,6′-d_2)	0.7		13.39
	1,4-	2,3,6-Me_3-Gal*p*(6,6′-d_2)	99.3		18.05
	Total		100.0	69.56	

[a] Sample was carboxyl-reduced with sodium borodeuteride, methylated, then converted into alditol acetates(6,6′-d_2).
[b] Relative molar ratio, calculated from the ratio of peak areas.
[c] Mol. % of the parent AMBG, calculated from the ratio of peak areas.

was assigned to C-5 of terminal Ara*f* and C-6 of terminal and 3-linked Gal*p*. Signals at δ 68.3 (C-5 of 5 and 2,5-linked Ara*f*) and signals at δ 71.6 (6-linked and 3,6-linked Gal*p*) were also assigned. The weaker signals at δ 63.6 were attributed to C-5 of terminal Xyl*p* (Duan, Wang, Dong, Fang, & Li, 2003). δ 178.6 was attributed to C-6 of the carboxyl in the units $\rightarrow$4)-α-D-Gal*p*A(1 $\rightarrow$ 2)-α-L-Rha*p*-(1 $\rightarrow$, δ 178.3 attributed to that in the units $\rightarrow$4)-α-D-Gal*p*A(1 $\rightarrow$ 4)-α-D-Gal*p*A(1 $\rightarrow$, and δ 173.5 attributed to carboxyl groups in ester-form. The resonances at δ 102.7, 81.2, 73.1, 70.8 and 70.6 were assigned to C-1, C-4, C-5, C-3 and C-2 of the repeating unit $\rightarrow$4)-α-D-Gal*p*A(1 $\rightarrow$, respectively (Iacomini et al., 2005).

Based on the results described above, it could be concluded that AMBG might possess a backbone of the average disaccharide of [$\rightarrow$4)-α-D-Gal*p*A(1 $\rightarrow$ 2)-α-D-Rha*p*-(1 $\rightarrow$], having a certain degree of methyl esterification. The side chains are attached at the ***O***-4 of Rha*p*

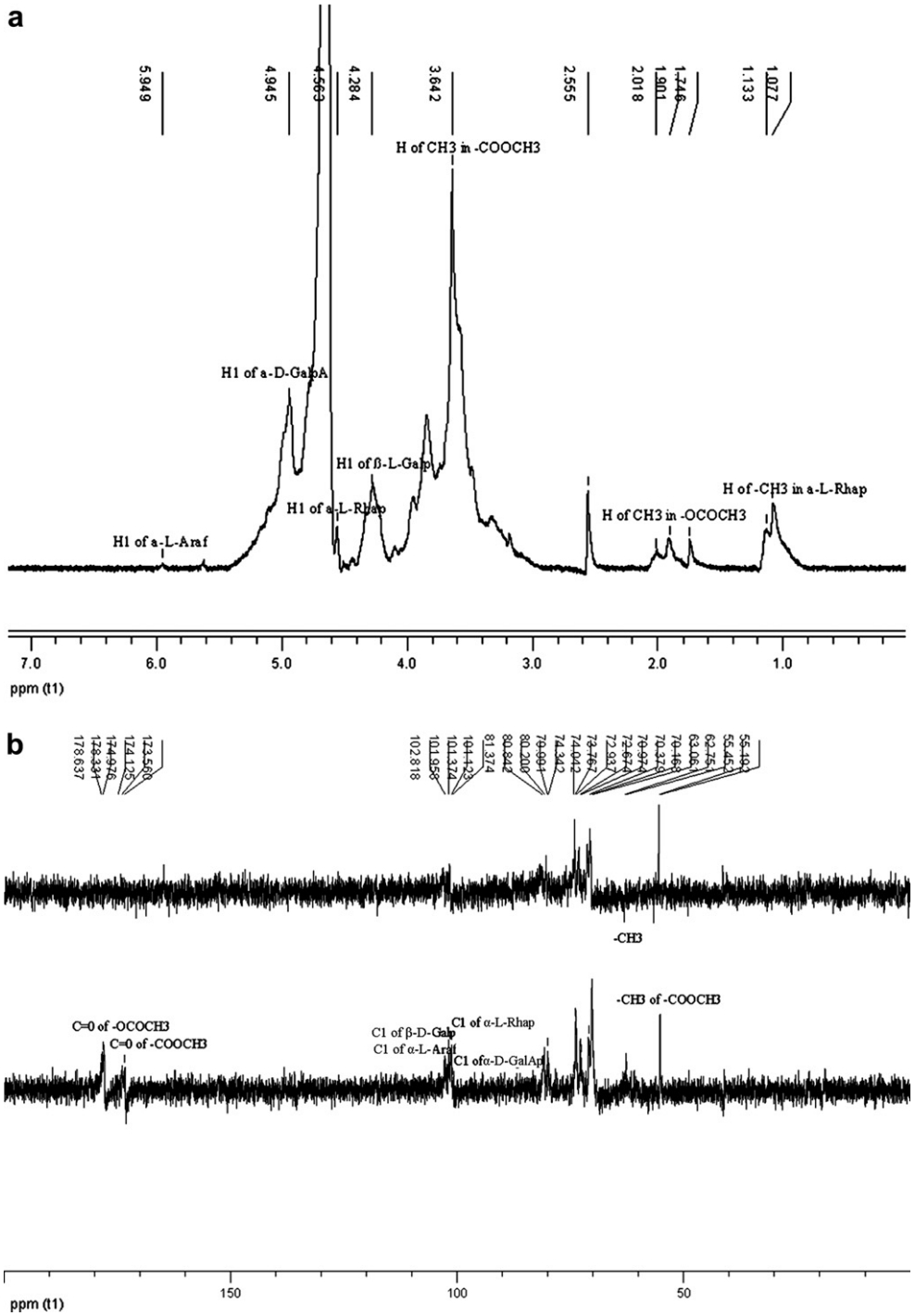

Fig. 6. (a) ^{1}H NMR spectrum of AMBG (400 MHz, 60 °C). (b) (^{13}C+BB135) NMR spectrum of AMBG (400 MHz, 60 °C).

residues, including β-(1 → 4)-linked Xyl*p* residues, and β-(1 → 3) and β-(1 → 6)-linked Gal*p* (galactan) residues. The highly branched α-(1 → 5) arabinan was attached to ***O***-2 of β-(1 → 4)-linked Xyl*p* and ***O***-3 of β-(1 → 6)-linked Gal*p* residues, forming arabinoxylan and arabinogalactan moieties, respectively. These partial structural features resemble those of the pectic polysaccharides isolated from the carrot, *Daucus carota* (Stevens & Selvendran, 1984), the seed of *Coix lacryma-jobi* L. var. ma-yuen (Yamada, Yanahira, Kiyohara, Cyong, & Otsuka, 1987), the root of *Angelica acutiloba* Kitagawa and the leaves of *Plantago major* L (Samuelsen et al., 1996). These acidic arabinogalactans contain a higher content of (1 → 3,6)-linked Gal*p* residues and/or contain some (1 → 4)-linked Gal*p* residues. Therefore, we could assume the structure of AMBG is as follows (Yamada, Kiyohara, Cyong, & Otsuka, 1987):

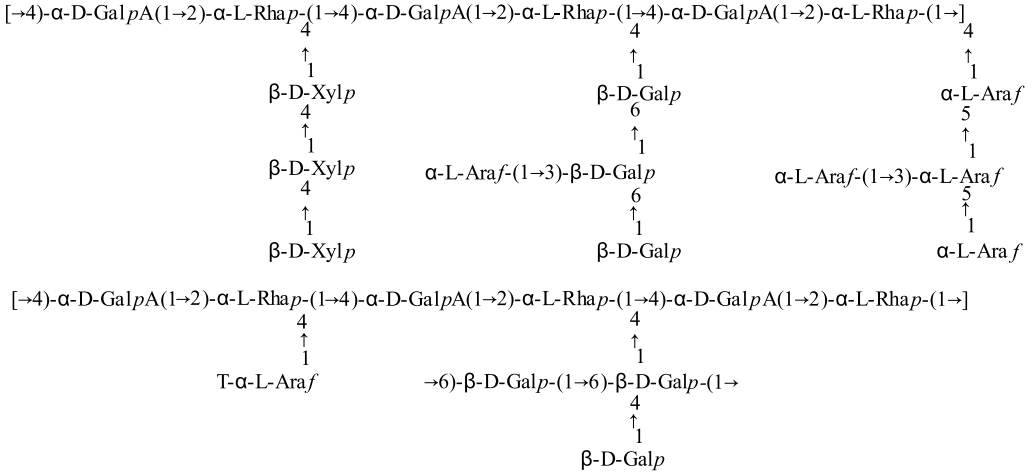

3.5. AFM of AMBG

AFM imaging of biopolymer was normally conducted in air or under a liquid in order to avoid excessive dehydration. A typical sample preparation procedure consisted of spreading of a dilute (1–10 μg/mL) polymer solution onto a freshly cleaved mica surface and successive air-drying under ambient pressure, temperature, and humidity. Fig. 7a and c shows a topographical AFM image of AMBG deposited from a 1 μg/mL aqueous solution. Only spherical lumps can be seen in Fig. 7a and c, the diameter and height of the lumps ranged from 5 to 10 nm and 1 to 4 nm, respectively. The heights of the spherical structures in Fig. 7a are much higher than that of a single polysaccharide chain (about 0.1–1 nm), suggesting that inter- and/or intra-molecular aggregation was involved. When deposition was made at a slightly higher polymer concentration (10 μg/mL), irregularly shaped large structure were formed together like worm (Fig. 7b and d), which suggested that AMBG could absorb water in the aqueous solution. On the other hand, due to the strong interaction between water molecules and the hydroxyl groups (–OH) of polysaccharides in the solution, AMBG released water slowly. Therefore, the fluidity of AMBG solution could be low because of network structure (Zhang et al., 2007).

3.6. Relationship between structure and rheology properties

The results from the viscosity measurements suggested that the viscosity (η) of the AMBG solution decreased with the increasing shear stress (τ) and exhibited a typical non-Newtonian pseudoplastic behavior. Due to its high galacturonic acid content AMBG has a lot of negatively charged carboxyl groups, which give AMBG molecules a very extended conformation in aqueous solution, and a high hydrodynamic volume. Moreover, AMBG is highly branched, which made AMBG molecules entangle with each other more easily, and show pseudoplastic behavior. A similar pseudoplastic behavior of viscosity was observed in case of an exopolysaccharide, EPS-WN9 from *Paenibacillus sp.* WN9 (Seo et al., 1999) and an extracellular polysaccharide from haloalkalophilic *Bacillus sp.* I-450 (Kumar, Joo, Choi, Koo, & Chang, 2004). The exponential decrease in the viscosity with the increasing shear rate (shear-thinning effect) was also noticed in case of rhamsam produced by *Alcaligenes sp.* which had the largest side chain, while gellan produced by *Pseudomonas elodea* exhibited the least shear-thinning, since this polysaccharide had no side chain in the backbone structure (Kwon, Foss, & Rha, 1987). The reduction in viscosity could also be attributed to polymer degradation due to the cleavage of glycosidic bonds within the polysaccharide structure (Ren, Ellis, Sutherland, & Ross-Murphy, 2003). The main Mango pectin SF2 was mostly polygalacturonic acid and type I rhamnogalacturonan. When analyzed by viscometric methods at steady shear, SF2 had a high viscosity, which might be explained by a mixture of charged polysaccharides perhaps with a different charge density and also by physical

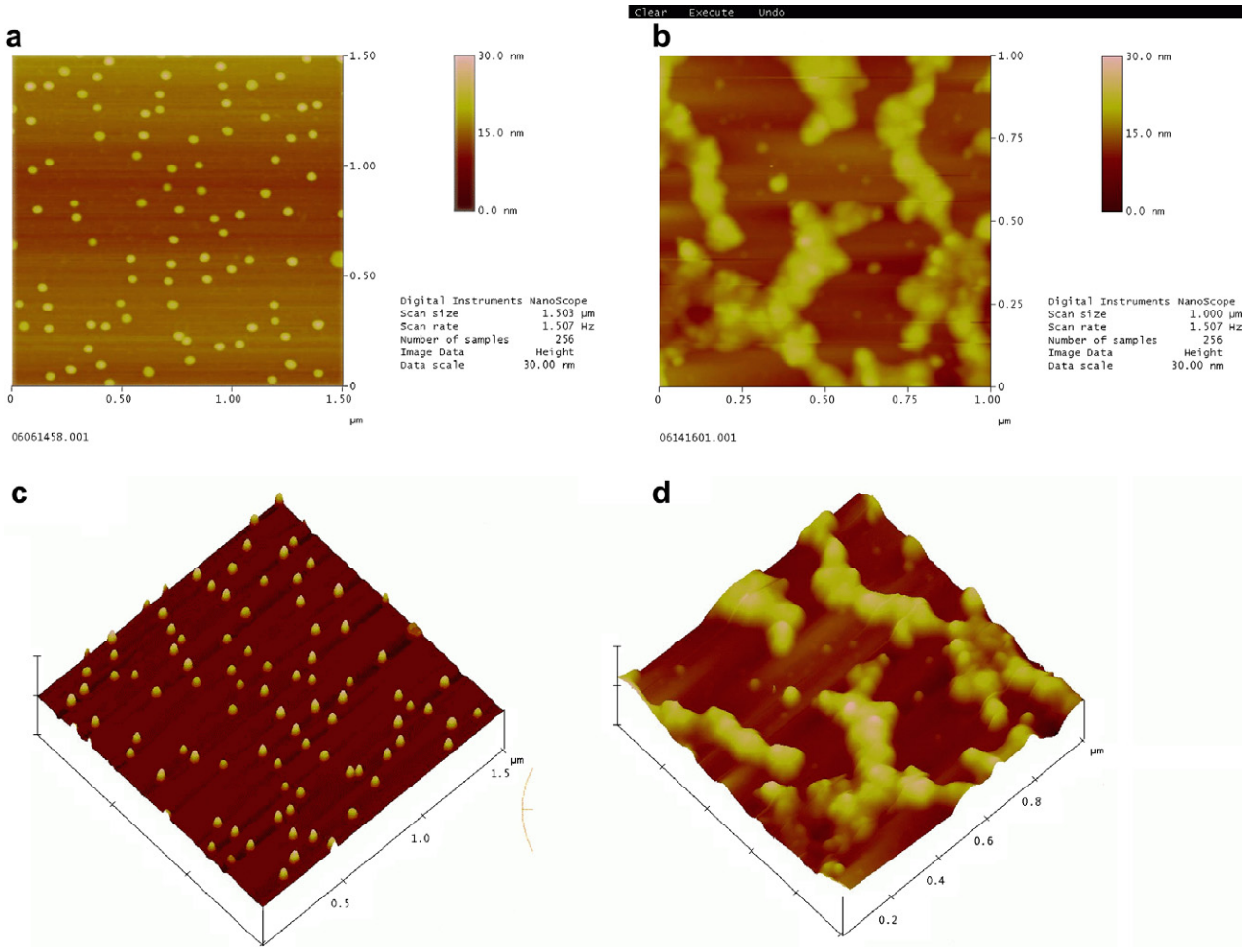

Fig. 7. Atomic force microscopy (AFM) planar (a and b) and cubic (c and d) images of molecular structure of AMBG from *Mesona Blumes* gum. The AMBG concentrations were 1 μg/mL (a and c) and 10 μg/mL (b and d). The atomic force microscopy was a Nano Scope IIIa instrument and was operated in the tapping-mode. The resulting imaging force was estimated to be 3–4 nN and the resonant frequency was about 2 kHz.

entanglements between the polysaccharide chains (Iagher, Reicher, & Ganter, 2002).

4. Conclusions

Two fractions were isolated from MBG, one was a neutral polysaccharide (NMBG) with a molecular weight of 5277 g/mol, the other was acidic polysaccharide (AMBG) with a molecular weight of 6566 g/mol. NMBG had no galacturonic acid but AMBG had it. NMBG solutions, 1–5% (w/w), all exhibited a Newtonian behavior and AMBG solutions, 1–5% (w/w), all exhibited a shear-thinning behavior in the shear rate range from 1 to 100 s^{-1}.

Chemical and spectral data support the conclusion that AMBG has a very complex structure; the backbone corresponds to a galacturono rhamnan; these residues are both 4-*O*-linked. The branches of the structure are composed of galactan, arabinan, xylan and its 4-*O*-methyl derivatives.

Data on the AFM images showed that AMBG molecules formed a spherical lump at 1 μg/mL, but gave a worm-like shape at 10 μg/mL. The pseudoplastic behavior of AMBG aqueous solution might be related to its highly charged carboxyl groups and large number of side chains.

References

Bushneva, O. A., Ovodova, R. G., Shashkov, A. S., & Ovodov, Y. S. (2002). Structural studies on hairy region of pectic polysaccharide from campion Silene vulgaris (Oberna behen). *Carbohydrate Polymers, 49*, 471–478.

Caili, F., Haijun, T., Tongyi, C., Yi, L., & Quanhong, L. (2007). Some properties of an acidic protein-bound polysaccharide from the fruit of pumpkin. *Food Chemistry, 100*, 944–947.

Ciucanu, I., & Kerek, F. (1984). simple and rapid method for the permethylation of carbohydrates. *Carbohydrate Research, 131*, 209–217.

Cozzolino, R., Malvagna, P., Spina, E., Giori, A., Fuzzati, N., Anelli, A., et al. (2006). Structural analysis of the polysaccharides from Echinacea angustifolia radix. *Carbohydrate Polymers, 65*, 263–272.

Duan, J., Wang, X., Dong, Q., Fang, J., & Li, X. (2003). Structural features of a pectic arabinogalactan with immunological activity from the leaves of Diospyros kaki. *Carbohydrate Research, 338*, 1291–1297.

Duan, J., Zheng, Y., Dong, Q., & Fang, J. (2004). Structural analysis of a pectic polysaccharide from the leaves of Diospyros kaki. *Phytochemistry, 65*, 609–615.

Fleury, P., & Lange, J. (1933). Determination of the periodate consumption of polysaccharides. *Journal of Pharmaceutical Chemistry, 17*, 196–208.

Gunning, A. P., Giardina, T. P., Faulds, C. B., Juge, N., Ring, S. G., Williams, G., et al. (2003). Surfactant mediated solubilisation of amylase and visualization by atomic force microscopy. *Carbohydrate polymers, 51*, 177–182.

Habibi, Y., Heyraud, A., Mahrouz, M., & Vignon, M. R. (2004). Structural features of pectic polysaccharides from the skin of Opuntia ficus-indica prickly pear fruits. *Carbohydrate Research, 339*, 1119–1127.

Iacomini, M., Serrato, R. V., Sassaki, G. L., Lopes, L., Buchi, D. F., & Gorin, P. A. (2005). Isolation and partial characterization of a pectic polysaccharide from the fruit pulp of Spondias cytherea and its effect on peritoneal macrophage activation. *Fitoterapia, 76*, 676–683.

Iagher, F., Reicher, F., & Ganter, J. L. (2002). Structural and rheological properties of polysaccharides from mango (Mangifera indica L.) pulp. *International Journal of Biological Macromolecules, 31*, 9–17.

Inngjerdingen, K. T., Debes, S. C., Inngjerdingen, M., Hokputsa, S., Harding, S. E., Rolstad, B., et al. (2005). Bioactive pectic polysaccharides from Glinus oppositifolius (L.) Aug. DC., a Malian medicinal plant, isolation and partial characterization. *Journal of Ethnopharmacology, 101*, 204–214.

Kirby, A. R., Gunning, A. P., & Morris, V. J. (1995). Imaging xanthan gum by atomic force microscopy. *Carbohydrate Research, 267*, 161–166.

Kjoniksen, A. L., Hiorth, M., & Nystrom, B. (2005). Association under shear flow in aqueous solutions of pectin. *European Polymer Journal, 41*, 761–770.

Kumar, C. G., Joo, H. S., Choi, J. W., Koo, Y. M., & Chang, C. S. (2004). Purification and characterization of an extracellular polysaccharide from haloalkalophilic Bacillus sp. I-450. *Enzyme and Microbial Technology, 34*, 673–681.

Kwon, B. D., Foss, P. A., & Rha, C. (1987). Rheological characteristics of high viscosity polysaccharides. In M. Yalpan (Ed.), *Industrial polysaccharides: Genetic engineering, structure/property relations and applications* (pp. 253–266). Amsterdam: Elsevier Science Publishers.

Lai, L. S., Liu, Y. L., & Lin, P. S. (2003). Rheological/textural properties of starch and crude hsian-tsao leaf gum mixed systems. *Journal of Food Science and Agriculture, 83*, 1051–1058.

Lai, L. S., & Lin, P. H. (2004). Application of decolorized hsian-tsao leaf gum to low-fat salad dressing model emulsions: Rheological study. *Journal of Food Science and Agriculture, 84*, 1307–1314.

Lai, L. S., Tung, J., & Lin, P. S. (2000). Solution properties of hsian-tsao (Mesona procumbent Hemsl) leaf gum. *Food Hydrocolloids, 14*, 287–294.

Li, X., Nakagawa, N., Nevins, D. J., & Sakurai, N. (2006). in the cell-wall polysaccharides of outer pericarp tissues of kiwifruit during development. *Plant Physiology and Biochemistry, 44*, 115–124.

Liu, C., Lin, Q., Gao, Y., Ye, L., Xing, Y., & Xi, T. (2007). Characterization and antitumor activity of a polysaccharide from Strongylocentrotus nudus eggs. *Carbohydrate Polymers, 67*, 313–318.

Ren, Y., Ellis, P. R., Sutherland, I. W., & Ross-Murphy, S. B. (2003). Dilute and semi-dilute solution properties of an exopolysaccharide from *Escherichia coli* strain S61. *Carbohydrate Polymers, 52*, 189–195.

Samuelsen, A. B., Paulsen, B. S., Wold, J. K., Otsuka, H., Kiyohara, H., Yamada, H., et al. (1996). Characterization of a biologically active pectin from Plantago major L. *Carbohydrate Polymers, 30*, 37–44.

Seo, W. T., Kang, G. G., Nam, S. H., Choi, S. D., Suh, H. H., & Kim, S. W. (1999). Isolation and characterization of a novel exopolysaccharide-producing Paenibacillus sp. WN9 KCTC 8951P. *Journal of Microbiology and Biotechnology, 9*, 820–825.

Shiga, T. M., & Lajolo, F. M. (2006). Cell wall polysaccharides of common beans (Phaseolus vulgaris L.) – Composition and structure. *Carbohydrate Polymers, 63*, 1–12.

Sims, I. M., & Newman, R. H. (2006). Structural studies of acidic xylans exuded from leaves of the monocotyledonous plants Phormium tenax and Phormium cookianum. *Carbohydrate Polymers, 63*, 379–384.

Singthong, J., Cui, S. W., Ningsanond, S., & Douglas, G. H. (2004). Structural characterization, degree of esterification and some gelling properties of Krueo Ma Noy (Cissampelos pareira) pectin. *Carbohydrate Polymers, 58*, 391–400.

Stevens, B. J., & Selvendran, R. R. (1984). Structural features of cell-wall polysaccharides of the carrot Daucus carota. *Carbohydrate Research, 128*, 321–333.

Taylor, R. L., & Conrad, H. E. (1972). Stoichiometric depolymerization of polyuronides and glycosaminoglycuronans to monosaccharides following reduction of their carbodiimide-activated carboxyl groups. *Biochemistry, 11*, 1383–1388.

Yamada, H., Yanahira, S., Kiyohara, H., Cyong, J., & Otsuka, Y. (1987). Characterization of anti-complementary acidic heteroglycans from the seed of Coix lacryma-jobi L. var. ma-yuen. *Phytochemistry, 26*, 3269–3275.

Yamada, H., Kiyohara, H., Cyong, J. C., & Otsuka, Y. (1987). Structural characterisation of an anti-complementary arabinogalactan from the roots of Angelica acutiloba kitagawa. *Carbohydrate Research, 159*, 275–291.

Yang, C. C., & Huang, S. H. (1990). The gel-forming properties and chemical compositions of the gum extract from leaf, stem and root of the hsian-tsao herb (Mesona Procumbent Hemsl). *Food Science (Taipei), 17*, 260–265.

Zhang, H., Yao, H., Chen, F., & Wang, X. (2007). Purification and characterization of glutamate decarboxylase from rice germ. *Food Chemistry, 101*, 1670–1676.

Zhang, J., Wu, J., Liang, J. Y., Hu, Z. A., Wang, Y. P., & Zhang, S. (2007). Chemical characterization of Artemisia seed polysaccharide. *Carbohydrate Polymers, 67*, 213–218.